Molecular Plant Pathology

MOLECULAR PLANT PATHOLOGY (2010) **11**(1), 105–119 DOI: 10.1111/J.1364-3703.2009.00579.X

The role of mitogen-activated protein (MAP) kinase signalling components and the Ste12 transcription factor in germination and pathogenicity of *Botrytis cinerea*

ASTRID SCHAMBER[1], MICHAELA LEROCH[1], JANINE DIWO[1], KURT MENDGEN[2] AND MATTHIAS HAHN[1,*]

[1]*Department of Biology, University of Kaiserslautern, PO Box 3049, 67653 Kaiserslautern, Germany*
[2]*Department of Biology, University of Konstanz, 78457 Konstanz, Germany*

SUMMARY

In all fungi studied so far, mitogen-activated protein (MAP) kinase cascades serve as central signalling complexes that are involved in various aspects of growth, stress response and infection. In this work, putative components of the yeast Fus3/Kss1-type MAP kinase cascade and the putative downstream transcription factor Ste12 were analysed in the grey mould fungus *Botrytis cinerea*. Deletion mutants of the MAP triple kinase Ste11, the MAP kinase kinase Ste7 and the MAP kinase adaptor protein Ste50 all resulted in phenotypes similar to that of the previously described BMP1 MAP kinase mutant, namely defects in germination, delayed vegetative growth, reduced size of conidia, lack of sclerotia formation and loss of pathogenicity. Mutants lacking Ste12 showed normal germination, but delayed infection as a result of low penetration efficiency. Two differently spliced *ste12* transcripts were detected, and both were able to complement the *ste12* mutant, except for a defect in sclerotium formation, which was only corrected by the full-sized transcript. Overexpression of the smaller *ste12* transcript resulted in delayed germination and strongly reduced infection. Bc-Gas2, a homologue of *Magnaporthe grisea* Gas2 that is required for appressorial function, was found to be non-essential for growth and infection, but its expression was under the control of both Bmp1 and Ste12. In summary, the role and regulatory connections of the Fus3/Kss1-type MAP kinase cascade in *B. cinerea* revealed both common and unique properties compared with those of other plant pathogenic fungi, and provide evidence for a regulatory link between the BMP1 MAP kinase cascade and Ste12.

*Correspondence: E-mail: hahn@rhrk.uni-kl.de

INTRODUCTION

Plant pathogenic fungi employ a great diversity of infection strategies. Nevertheless, they share similarities during invasion of living plant tissue, such as the formation of appressoria and the ability to penetrate plant cell walls. Appropriate timing of germination and location of the site of penetration is achieved by the perception of various host-derived signals. For instance, physical signals, such as surface topography and surface hydrophobicity, and chemical signals, such as cutin or wax components and sugars, have been identified as triggers of spore germination and appressorium formation (Doehlemann *et al*., 2006; Mendgen *et al*., 1996). Although the mechanism of perception of these stimuli is still poorly understood, conserved signal transduction elements have been shown to be involved in pathogenic differentiation. Signalling pathways involving heterotrimeric G proteins, cyclic adenosine monophosphate (cAMP) and cAMP-regulated protein kinases have been shown to be required for appressorium formation and infection in a variety of fungi, such as *Magnaporthe grisea* (Xu and Hamer, 1996), *Colletotrichum* spp. (Takano *et al*., 2000) and *Botrytis cinerea* (Schumacher *et al*., 2008). Mitogen-activated protein kinases (MAPKs) also play a central role in the transduction of extracellular signals. They work in a cascade of hierarchical components, namely MAPK kinase kinase, MAPK kinase and MAPK. In *Saccharomyces cerevisiae*, the MAPK cascade Ste11, Ste7 and Fus3/Kss1 has been shown to be required for both mating and filamentous growth (Gustin *et al*., 1998). In plant pathogenic fungi, MAPKs homologous to Fus3 and Kss1 have been shown to be essential for appressorium formation and infection, for instance in *M. grisea* (PMK1), *Colletotrichum lagenarium* (CMK1) and *Pyrenophora teres* (CMK1) (for a review, see Zhao *et al*., 2007). In *M. grisea*, further components of the PMK1 MAPK cascade have been characterized, and their structural and functional interactions have been analysed (Park *et al*., 2006; Zhao and Xu, 2007; Zhao *et al*., 2005).

In *S. cerevisiae*, the activity of the transcription factor Ste12 is controlled by the Fus3/Kss1 MAPK cascade, but requires several further interacting components. Activation by mating pheromones occurs only in cells containing a Ste12/Dig1/Dig2 complex. It is achieved by Fus3- or Kss1-mediated phosphorylation of the two Ste12 inhibitors, Dig1 and Dig2, thereby relieving their inhibitory activity (Chou *et al*., 2006). In contrast, the activation of genes involved in filamentation depends on the Tec1/Ste12/Dig1 complex, containing the Tec1 transcription factor. The availability of an active complex is regulated in a Fus3- and Kss1-dependent manner by the modulation of Tec1 synthesis and stability (Chou *et al*., 2006).

In the plant pathogens *M. grisea*, two *Colletotrichum* spp. and *Cryphonectria parasitica*, Ste12 homologues have been shown to be required for infection. Ste12-deficient mutants are either non-pathogenic or strongly reduced in virulence, and show defects in penetration (Deng *et al*., 2007; Hoi *et al*., 2007; Park *et al*., 2002). Ste12 proteins from filamentous ascomycetes differ from yeast Ste12 by the presence of two C-terminal, tandemly arranged C_2H_2 zinc finger domains. These do not seem to be required for DNA binding, but have been shown to be involved in the activity of Ste12 (Hoi *et al*., 2007; Park *et al*., 2004). In plant pathogenic fungi, no clear evidence yet exists on whether or not the activity of Ste12 is under the control of the Fus3/Kss1-type MAPK pathway. In the saprophytic fungus *Neurospora crassa*, there is evidence for such a regulatory link, as mutants defective in the MAPK *mak-2* and the Ste12 homologue *pp-1* show similar phenotypes. In addition, microarray hybridization studies have revealed many genes that were found to be dependent on both *mak-2* and *pp-1* (Li *et al*., 2005).

The necrotrophic fungus *B. cinerea* preferentially invades soft tissue and ripening fruits of a large variety of host plants (Williamson *et al*., 2007). The penetration of host cells can occur by germinated conidia, usually after the formation of appressoria-like hyphal swellings, which are usually not delineated from the germ tube by a septum. Penetration starting from saprophytic mycelium is initiated via hyphal aggregations, called infection cushions (Williamson *et al*., 2007). Similar to other fungi, the Fus3/Kss1-type BMP1 MAPK is essential for pathogenesis: Δ*bmp1* mutants fail to differentiate appressoria-like structures, resulting in a non-pathogenic phenotype, and are unable to germinate on hydrophobic surfaces in the absence of nutrients (Doehlemann *et al*., 2006; Zheng *et al*., 2000). In this paper, we describe further components of the MAPK cascade in *B. cinerea*, namely Ste11, Ste7 and Ste50, and present a detailed analysis of the gene encoding Ste12. Although the mutant phenotypes for the MAPK components and for Ste12 showed only partial similarities, we identified a gene, *gas2*, which requires both BMP1 and Ste12 for expression.

RESULTS

Identification of putative components of the BMP1-related MAPK cascade

In the *B. cinerea* genome database at the National Center for Biotechnology Information (NCBI) (http://www.ncbi.nlm.nih.gov), homologues to genes encoding the *S. cerevisiae* and *M. grisea* components of the Fus3/Kss1-type MAPK cascade were identified, namely MAPKKK Ste11, MAPKK Ste7 and the adaptor protein Ste50. The gene product of *Bc-ste11* is a predicted protein of 957 amino acids, with 63% identity to *M. grisea* Mst11 and 23% identity to yeast Ste11. *Bc-ste7* encodes a protein of 520 amino acids, with 65% identity to *M. grisea* Mst7 and 22% identity to yeast Ste7. Transcription of *Bc-ste50* leads to a protein of 501 amino acids, with 62% identity to *M. grisea* Mst50 and only 17% identity to yeast Ste50. The homologues of *B. cinerea* and *M. grisea*, as well as those of other filamentous ascomycetes (not shown), are much more similar to each other than to those of yeast. Predictions of Expasy Prosite (http://www.expasy.ch/prosite) revealed that the *B. cinerea* proteins contain the same characteristic domains as their *M. grisea* homologues. Amino acids 60–129 in Ste11 and 66–129 in Ste50 are putative sterile α motif (SAM) domains, which are known to be involved in the interaction of these two proteins and are essential for appressorium formation in *M. grisea* (Park *et al*., 2006). Amino acids 292–382 in Ste11 and amino acids 367–465 in Ste50 are Ras-association (RA) domains, which are also involved in appressoria formation. Based on these structural similarities, *B. cinerea* Ste11, Ste7 and Ste50 were assumed to represent functional orthologues to the respective *M. grisea* and yeast proteins.

Construction and characterization of *B. cinerea* mutants lacking MAPK components

To investigate the role of *B. cinerea* Ste11, Ste7 and Ste50, knock-out mutants were constructed, in which the coding regions of the respective genes were replaced by a hygromycin resistance cassette (see Experimental procedures). Initial identification of the mutants (three independent knock-out mutants per gene) was performed by polymerase chain reaction (PCR) (data not shown) and confirmed by Southern hybridization analysis (Fig. S1A, see Supporting Information).

The deletion mutants were tested for vegetative growth, in comparison with the previously published Δ*bmp1* MAPK mutant (Doehlemann *et al*., 2006) and the wild-type (wt) strain. Radial growth of all MAPK mutants (Δ*bmp1*, Δ*ste7*, Δ*ste11* and Δ*ste50*) was retarded to similar degrees (Fig. S2A, see Supporting Information). Depending on the medium used, the growth reduction relative to the wt strains was in the range 30%–70%.

In the presence of 0.5 M NaCl or 1.0 M sorbitol, the growth of the wt and mutant strains was inhibited to a similar relative extent (data not shown). Therefore, despite their growth defect, the mutants were not particularly sensitive to high osmolarity and salt stress conditions. Furthermore, the MAPK mutants showed reduced proliferation of the aerial mycelium, which appeared more compact than the wt aerial mycelium (Fig. 1A).

As already reported for the Δ*bmp1* mutant, conidia of all MAPK mutants were significantly smaller and more spherical than wt conidia (Doehlemann *et al*., 2006). The calculated volume of mutant conidia was only little more than one-half of the volume of wt conidia (Figs 1B and S2B, see Supporting Information). Furthermore, the reduced size of the conidia of the MAPK mutants was correlated with a smaller number of nuclei per conidium. For example, conidia of the Δ*bmp1* mutant contained only 2.1 ± 0.1 nuclei, whereas wt conidia contained an average of 3.7 ± 0.1 nuclei. The smaller number of nuclei is probably a result of the reduced size of the conidia of the mutants. When wt conidia of different sizes were inspected for their content of nuclei, a similar correlation between conidial size and number of nuclei was observed.

The Δ*bmp1* mutant has previously been shown to be unable to form sclerotia (Doehlemann *et al*., 2006). Similarly, no sclerotia formation was observed in the Δ*ste7*, Δ*ste11* and Δ*ste50*

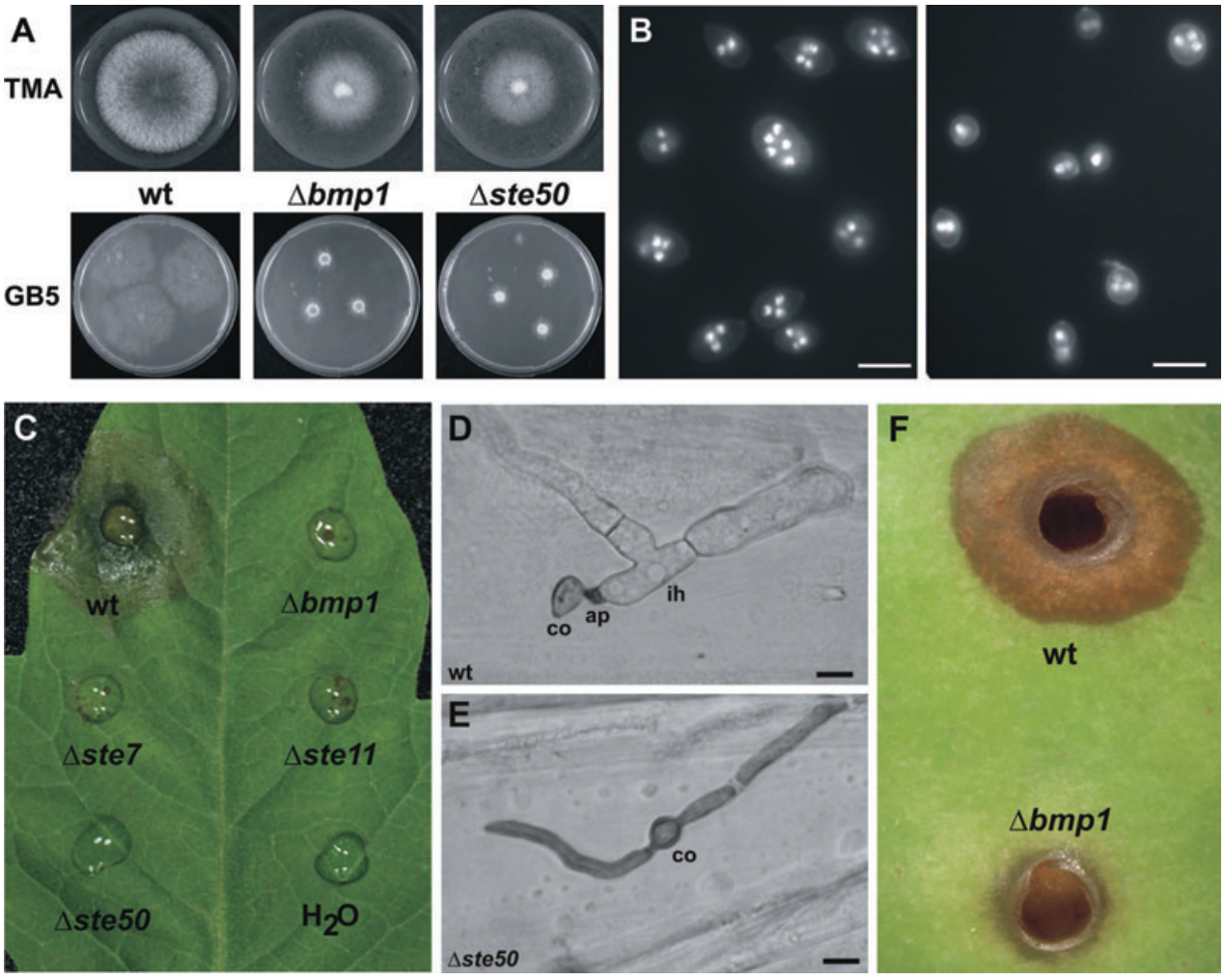

Fig. 1 Phenotypes of mitogen-activated protein kinase (MAPK) mutants. (A) Mycelial growth of wild-type (wt), Δ*bmp1* and Δ*ste50* mutants on tomato malt extract agar (TMA) and Gamborg's B5 (GB5) minimal medium [3 days post-inoculation (dpi)]. (B) Fluorescence micrographs showing conidia of wild-type (left) and Δ*bmp1* mutant (right) with Hoechst 33342-stained nuclei. Bars, 10 μm. (C) Infection test with detached tomato leaves [72 h post-inoculation (hpi)]. Note some scattered necrotic spots at inoculation sites of some of the MAPK mutants. (D, E) Penetration of germinated wt (D) and Δ*ste50* (E) conidia into onion epidermis cells (16 hpi). wt conidia (co) germinate with a short germ tube and develop an appressorium (ap) and thick, branched infection hyphae (ih). In contrast, appressoria and infection hyphae were never observed in the Δ*ste50* mutant or in the other MAPK mutants. Bars, 10 μm. (F) Infection test on a wounded apple (72 dpi).

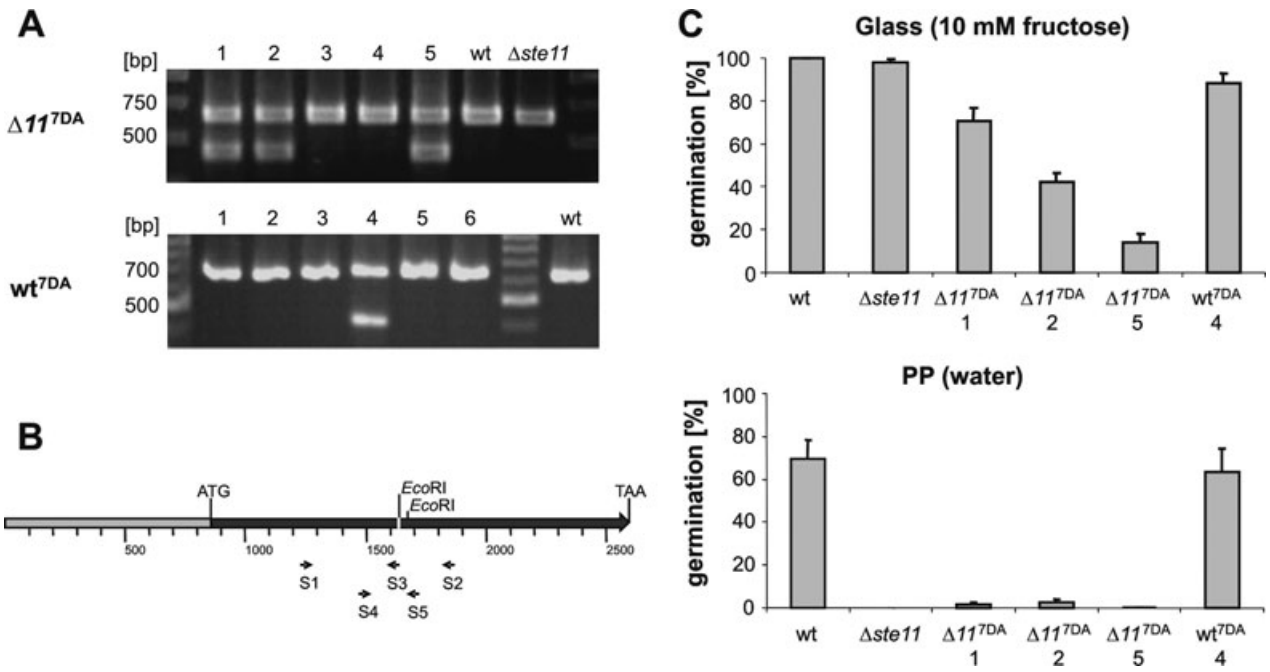

Fig. 2 Molecular and phenotypic analysis of *Botrytis cinerea* strains expressing *ste7*^{DA}. (A) Molecular confirmation of wild-type (wt) and Δ*ste11* strains transformed with *ste7*^{DA}. Genomic DNA was amplified using the three primers Bst7-S1, Bst7-S2 and Bst7-S3. In the case of the presence of the *ste7*^{DA} allele, two bands appeared on agarose gels. (B) Map of the *ste7*^{DA} construct used for transformation, with 846 bp of upstream sequence (grey) and the complete coding region (black). The mutated sequence is indicated in white with the newly introduced *Eco*RI site, 37 bp left of a natural *Eco*RI site. Primers are indicated by arrows. (C) Germination tests on glass slides in 10 mM fructose on glass and in water on a hydrophobic surface (24 h post-inoculation).

mutants (not shown). In contrast, these mutants produced microconidia (which serve as spermatia during sexual reproduction) under conditions in which the wt did not form any microconidia [tomato malt extract agar (TMA) medium, 20 °C, dark; not shown].

We have previously shown that the conidia of Δ*bmp1* mutants have a specific germination defect (Doehlemann *et al*., 2006). We therefore tested all MAPK mutants for germination (Fig. S2B, see Supporting Information). In 10 mM fructose on glass surfaces, almost complete germination was observed after 24 h in the wt and mutants. In contrast, in pure water on hydrophobic surfaces, such as polypropylene foil, the MAPK mutants were completely unable to germinate, whereas the wt showed a high germination rate. In full media, such as HA, germination of the mutants and the wt occurred with equally high efficiency (not shown). These data show that all MAPK mutants have the same germination defect on hydrophobic surfaces in water (Doehlemann *et al*., 2006).

The MAPK mutants were tested for infection using detached tomato leaves. In contrast with the wt, which started to form spreading lesions on tomato leaves after approximately 1 day, the MAPK mutants were unable to cause lesions, except for sporadic necrotic spots (Fig. 1C). The penetration ability of these mutants was studied on dead onion epidermis cell layers. Although wt conidia formed short germ tubes which quickly penetrated into the epidermal cells, the MAPK mutants formed long hyphae which failed to show any penetration attempts or terminal swellings (Fig. 1D,E; Doehlemann *et al*., 2006). When infection tests were performed with wounded apples, the lesions formed by the mutants expanded much more slowly than those induced by the wt strain (Fig. 1F).

Phenotypes of strains carrying a dominant active *ste7* allele (*ste7*^{DA}) in wt and Δ*ste11* mutant

To confirm the functional hierarchy of the MAPK components Ste11, Ste7 and BMP1, we used site-directed mutagenesis to create *ste7*^{DA}. A construct containing *ste7*^{DA}, including 846 bp of the *ste7* promoter, was transformed into both a *B. cinerea* Δ*ste11* mutant and the B05.10 wt strain. When PCR was performed with the three primers Bst7-S1, Bst7-S2 and Bst7-S3, two products were obtained in one of the wt transformants (no. 4) and in three of the Δ*ste11* transformants (nos. 1, 2, 5). This confirmed the genomic integration of *ste7*^{DA}, as Bst7-S3 binds only at the mutated site (Fig. 2A,B). Using primers Bst7-S4 and Bst7-S5, a smaller PCR product was amplified (Fig. 2B) and digested with *Eco*RI, resulting in different fragments in the case of *ste7*^{DA} or wt alleles (data not shown). Because all transfor-

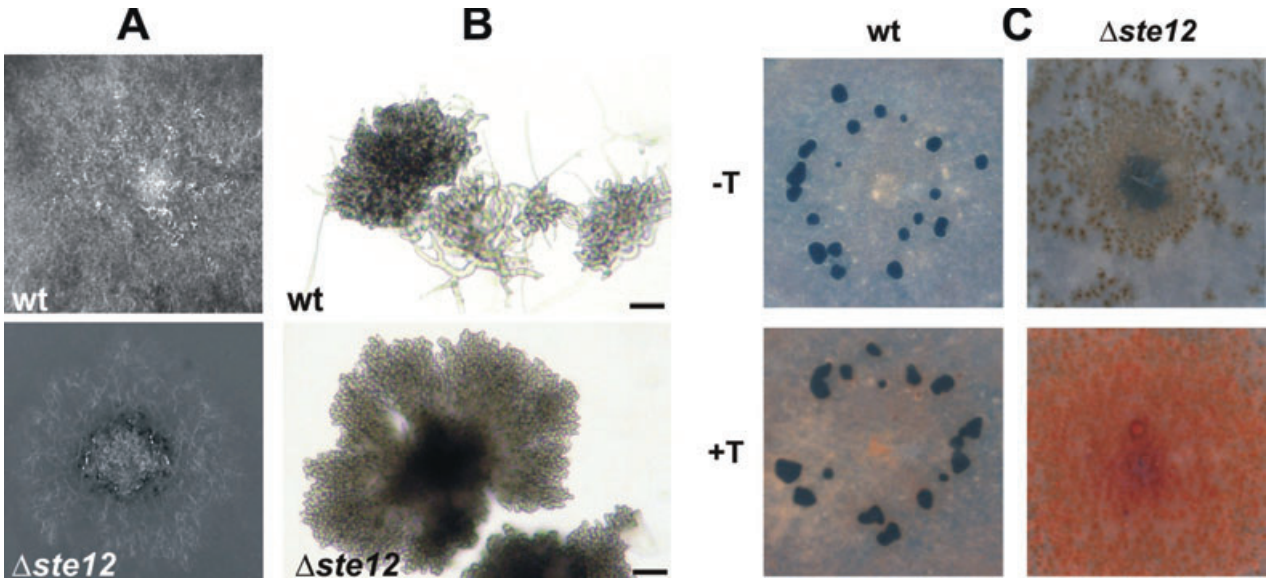

Fig. 3 Growth phenotype of *Botrytis cinerea* Δ*ste12* mutant on solid minimal medium. (A) After 3 days of growth, the mutant shows melanization of mycelium around the inoculation site. (B) Microscopic picture [3 days post-inoculation (dpi); bars, 200 μm]. The wild-type (wt) forms small aggregates which do not expand much further, whereas the larger aggregates of the *Dste12* mutant expand further and show increasing melanization. (C) Melanin production of wt and Δ*ste12* during growth on minimal medium (10 dpi). In the presence of 10 μg/mL tricyclazole, the Δ*ste12* mycelium formed much more orange–pink pigmentation than did wt mycelium. Melanized sclerotia are only observed in the wt, irrespective of the presence of tricyclazole.

mants showed both restriction patterns, we concluded that the *ste7*^{DA} construct was integrated ectopically into the transformants, in addition to the resident *ste7* wt allele. Expression of the *ste7*^{DA} allele in the transformants was confirmed by real-time PCR (RT-PCR), although, in the wt transformant, expression appeared to be low (Fig. S3, see Supporting Information).

When the strains transformed with *ste7*^{DA} were tested for germination, the wt transformant behaved almost normally, except for a minor reduction in the efficiency of sugar-induced germination on glass surfaces (Fig. 2C). However, the three Δ*ste11* transformants showed a stronger reduction in the sugar-induced germination rate, when compared with both wt and Δ*ste11* mutant conidia. However, on a hydrophobic surface in water, which does not allow any germination of Δ*ste11* conidia, very low but reproducible germination (up to 3%) was observed with conidia of Δ*ste11* mutants expressing *ste7*^{DA}. Germination in the presence of HA medium was normal [100% at 24 h post-inoculation (hpi)], showing that the general fitness of the spores was not affected. The infection behaviour of the transformants expressing *ste7*^{DA} was similar to that of the non-transformed strains, i.e. the transformed wt strain showed normal infection, whereas the transformed Δ*ste11* strains showed no infection of tomato leaves (data not shown). Taken together, the expression of the *ste7*^{DA} allele very weakly restored the defect in germination on hydrophobic surfaces, but not the non-pathogenic phenotype of Δ*ste11* conidia.

Characterization of the gene encoding the Ste12 transcription factor

In addition to the genes encoding putative MAPK components, *ste12* was identified in the *B. cinerea* genome sequence. It encodes a homologue to yeast Ste12 and *M. grisea* Mst12 transcription factors and Ste12-like proteins of other ascomycetes. The predicted Ste12 protein is 704 amino acids long and shows 72% identity to *M. grisea* Mst12, but only 19% identity to yeast Ste12. For functional analysis, *B. cinerea ste12* deletion mutants were constructed and confirmed by Southern hybridization analysis (Fig. S1B, see Supporting Information). Radial growth of the Δ*ste12* mutants was slightly retarded to 92 ± 2.5% on TMA, to 53 ± 3.7% on HA and to 60 ± 4.3% on Gamborg's B5 (GB5) agar plates, in comparison with wt. In contrast, the complemented Δ*ste12* mutant showed similar growth rates compared with the values of the wt strain (12.3 ± 0.3 mm/day on TMA, 8.0 ± 0.7 mm/day on HA, 10.9 ± 0.6 mm/day on GB5 agar plates).

A peculiar behaviour of the Δ*ste12* mutant on solid minimal medium was the formation of dark aggregates on the surface of agar medium (Fig. 3A). Microscopic analysis showed that, in comparison with small hyphal aggregates of the wt, the Δ*ste12* mutant formed larger and much darker mycelial clumps (Fig. 3B). The dark pigment was bound to the cell walls of the hyphae and could not be extracted by detergents or organic

solvents. To test whether this pigment was melanin, colonies of wt and Δ*ste12* mutant grown on HA agar were treated with the melanin biosynthesis inhibitor tricyclazole (Bell and Wheeler, 1986). In the presence of 10 μg/mL tricyclazole, no dark pigment was observed in the *ste12* mutant; instead, the *ste12* hyphae and, to a lesser extent, wt hyphae showed bright orange to pink pigmentation (Fig. 3C). Similar pigments have been described as the melanin precursors flaviolin and 2-hydroxyjuglone that accumulate in *M. grisea* hyphae after tricyclazole treatment (Woloshuk *et al*., 1981). Germination of the Δ*ste12* mutant did not show any differences to the wt (data not shown). However, the Δ*ste12* mutant displayed a defect in sclerotia formation. No sclerotia were formed under standard conditions (GB5 agar, incubation in the dark at 20 °C for 10 days), whereas, at 0 and 4 °C, a few normal-looking sclerotia appeared after 4 weeks of incubation (data not shown).

When inoculated on tomato leaves, Δ*ste12* mutants showed reduced lesion formation (Fig. 4A). Primary lesions became visible with a delay of about 1 day compared with wt induced lesions. Lesions induced by the Δ*ste12* mutant appeared only sporadically under the inoculation droplets, indicating a low efficiency of penetration. Furthermore, radial lesion expansion by the Δ*ste12* mutant was slower (2.3 ± 0.1 mm/day vs. 3.5 ± 0.1 mm/day in the wt). No differences in lesion formation from the wt strain were observed with the complemented Δ*ste12* mutant and an ectopic transformant (Fig. 4A). To reveal the reason for the delay in primary lesion formation, early infection stages of the Δ*ste12* mutant were analysed microscopically. On heat-killed onion epidermis layers, the mutant formed larger appressoria than the wt, but penetration was never observed (Fig. 4B,C). On tomato leaves, successful invasion of the Δ*ste12* mutant into epidermal cells was observed very rarely. Instead, the mutant hyphae formed aggregations of hyphae with appressoria-like thickenings, apparently as a consequence of repeated, unsuccessful penetration attempts (Fig. 4E). Using scanning electron microscopy, repeated formation of non-functional, malformed appressoria by Δ*ste12* mutants on bean leaves was evident (Fig. 4F,G).

Ste12 is transcribed to two alternatively spliced mRNAs

Similar to other fungal Ste12 homologues, Bc-Ste12 contains a conserved N-terminal homeodomain (residues 59–203), believed to be involved in DNA binding (Vallim *et al*., 2000). Furthermore, it contains two tandemly arranged C_2H_2 zinc finger domains near the C-terminus (residues 572–596 and 602–624) that are conserved in Ste12 homologues of filamentous ascomycetes and basidiomycetes, but not present in yeast Ste12 (Fig. 5A–C).

In *C. lindemuthianum*, two splice variants of *Cl-ste12* transcripts have been described (Hoi *et al*., 2007). A similar splicing mechanism was observed in *B. cinerea*: by skipping of the 84-bp exon 4, a shortened version of the *ste12* mRNA, called *ste12ΔE4*, was identified, which encodes a smaller protein lacking 28 amino acids (residues 592–619) of the protein encoded by the full-sized *ste12* mRNA. Thus, *ste12ΔE4* encodes a single chimeric zinc finger domain consisting of the N-terminal 20 amino acids of the first and the C-terminal five amino acids of the second zinc finger domains (Fig. 5B).

Using quantitative RT-PCR, the relative abundance of the two alternatively spliced *ste12* transcripts was determined. When RNA samples from different stages of *B. cinerea* development were analysed, the expression of the full-sized *ste12* transcript was always higher than the expression of the *ste12ΔE4* transcript (Fig. 6). The overall *ste12* transcript levels did not change markedly relative to those of constitutively expressed control transcripts during different stages of germination and hyphal growth. During necrotrophic growth in tomato leaves, *ste12* transcript levels were low at 24 hpi, but reached levels similar to those of axenically grown hyphae at 48 hpi. The relative abundance of the full-sized *ste12* transcript relative to the *ste12ΔE4* transcript was higher during *in planta* growth than during saprophytic growth, especially at 48 hpi. The total expression levels of *ste12* in the Δ*bmp1* mutant were not significantly altered relative to those in the wt (data not shown).

ste12ΔE4 is able to complement most of the defects of Δ*ste12* mutants, but its overexpression has negative effects

In *C. lindemuthianum*, overexpression of the *ste12ΔE3* transcript has been shown to suppress invasive growth in both *C. lindemuthianum* and, heterologously expressed, in baker's yeast (Hoi *et al*., 2007). In order to reveal whether the *B. cinerea ste12ΔE4* transcript has similar properties, we performed complementation studies with the Δ*ste12* mutant by generating transformants with cDNA constructs encoding either the full-sized (*fs*) *ste12* transcript or the *ste12ΔE4* transcript. RT-PCR analyses confirmed that the transformants expressed only one *ste12* transcript (Fig. 7, Δ*ste12* + Δ*E4* or Δ*ste12* + *fs*). Both constructs led to full restoration of the wt phenotype with regard to a lack of melanized mycelium, normal penetration and full pathogenicity, except for sclerotia formation which was only complemented by the full-sized transcript. The expression of the full-sized Δ*ste12* transcript in the complemented Δ*ste12* mutant was higher than in the wt, but this had no effect on germination and infection. To detect possible negative effects of *ste12ΔE4* expression, we also transformed the wt strain with *ste12ΔE4*. Three transformants were obtained which contained

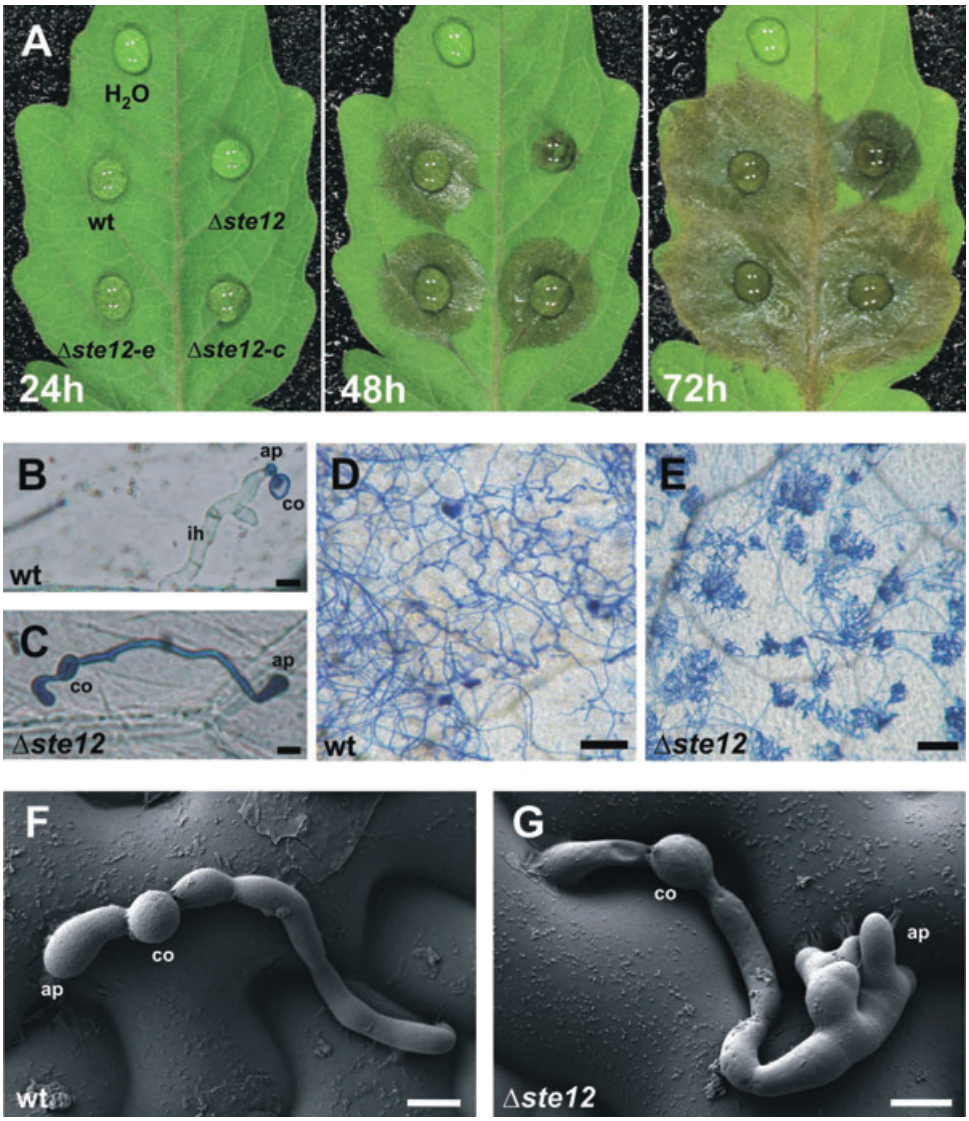

Fig. 4 Infection behaviour of *Botrytis cinerea* wild-type (wt) and Δ*ste12* mutants. (A) Infection of tomato leaves with wt, Δ*ste12*, an ectopic transformant (Δ*ste12-e*) and a complemented strain (Δ*ste12-c*) at 1–3 days post-inoculation (dpi). First, primary lesions are visible in the wt, ectopic and complemented mutants at 24 hours post-inoculation (hpi), but only after 2 days in the Δ*ste12* mutant, and secondary lesions spread more slowly in the Δ*ste12* mutant. (B, C) Penetration of wt and Δ*ste12* on onion epidermis at 20 hpi. wt conidia form short germ tubes and small appressoria, which penetrate quickly and form wide infection hyphae that show little trypan blue staining. In contrast, Δ*ste12* conidia form germ tubes of variable length, which show large appressoria but no successful penetration (bar, 10 μm). (D, E) Development of wt and Δ*ste12* mutant on tomato leaves (40 hpi). The wt penetrates the host cells with single hyphae. In contrast, the hyphae of the Δ*ste12* mutants form hyphal aggregates which do not seem to penetrate (bars, 100 μm). (F, G) Scanning electron micrographs showing infection structures of wt and Δ*ste12* mutant on the surface of bean leaves (bar, 10 μm). Note the formation of multiple malformed appressoria in the Δ*ste12* mutant. ap, appressorium; co, conidium.

ste12ΔE4 integrated ectopically in addition to wt *ste12* (data not shown). All transformants showed strongly reduced levels of the full-sized *ste12* transcript, but much higher levels of the *ste12ΔE4* transcript. Their infection behaviour ranged from delayed infection (nos. 0 and 5) to no infection at all (no. 1). The two transformants with highest *ste12ΔE4* expression (nos. 1 and 5) had strongly melanized mycelium, similar to the Δ*ste12* mutant. These negative effects were not observed when *ste12ΔE4* was expressed in the Δ*ste12* mutant, despite the fact that no full-sized transcript was detected either. Thus, the *ste12ΔE4*-encoded protein is almost fully functional if expressed at moderate levels, but its overexpression seems to have negative effects similar to or even more drastic than those of the Δ*ste12* mutant.

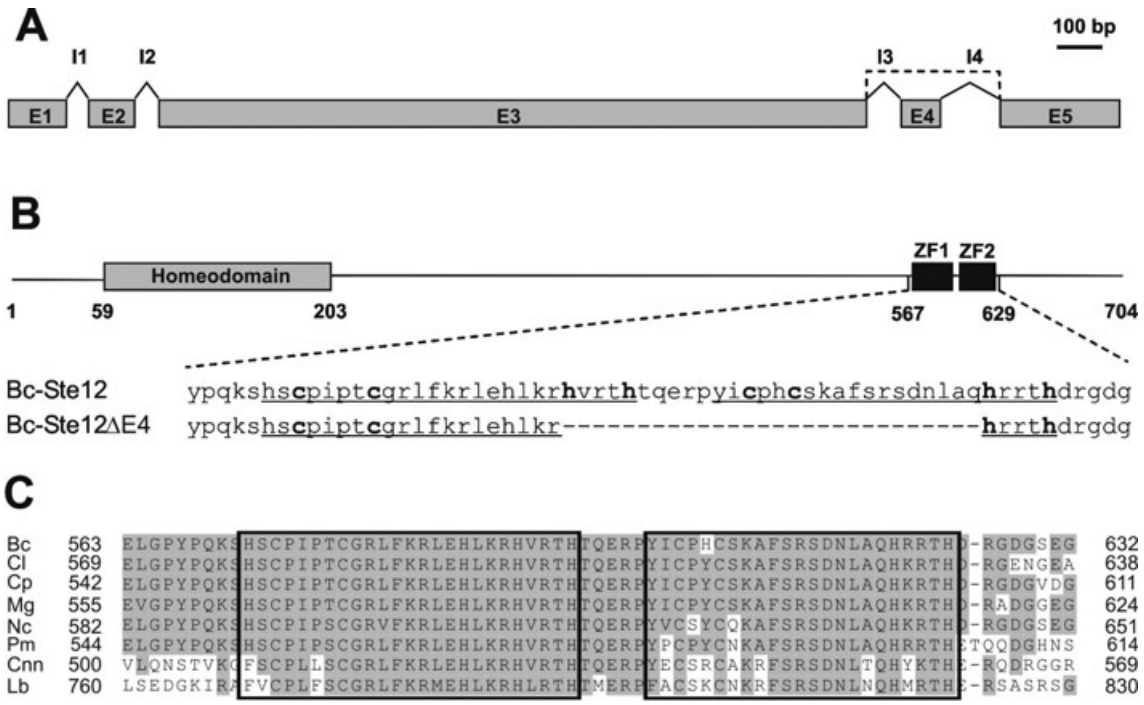

Fig. 5 Alternative splicing of *Botrytis cinerea ste12* transcripts leads to two different Ste12 proteins. (A) Organization of exons (E1–E5) and introns (I1–I4) in *ste12*. The broken line indicates the alternative splicing by exon skipping, leading to the shortened *ste12ΔE4* transcript. (B) Structures of the predicted Ste12 and Ste12ΔE4 proteins, showing the positions of the homeodomain region and two adjacent zinc finger domains (ZF1 and ZF2, underlined). Alternative splicing results in a shortened protein (Ste12ΔE4) containing only one zinc finger domain. Numbers indicate amino acid positions; conserved cysteine and histidine residues are shown in bold. (C) Alignment of the duplicate zinc finger region in fungal Ste12 proteins. Bc, *B. cinerea* (FJ374678); Cl, *Colletotrichum lindemuthianum* (CAD30840); Cnn, *Cryptococcus neoformans* var. *neoformans* (AAC01955); Cp, *Cryphonectria parasitica* (ABE67104); Lb, *Laccaria bicolor* (XP_001886200); Mg, *Magnaporthe grisea* (AAL27626); Nc, *Neurospora crassa* (XP_957811); Pm, *Penicillium marneffei* (AAK21854).

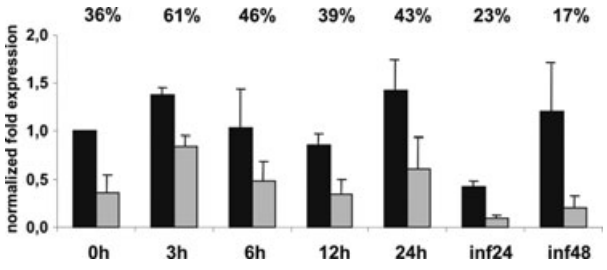

Fig. 6 Abundance of two *ste12* splicing variants in *Botrytis cinerea*. Quantitative real-time polymerase chain reaction (RT-PCR) data for full-sized *ste12* (black) and *ste12ΔE4* (grey) transcripts are shown at different times of germination (hours post-inoculation, hpi), and during growth in tomato leaf tissue (inf) at 24 and 48 hpi. The numbers at the top indicate the relative expression of the *ste12ΔE4* transcript (percentage of total *ste12* transcript levels).

The *gas2* gene is not required for infection but a target of BMP1 and Ste12

In *M. grisea*, two genes encoding similar proteins (Gas1 and Gas2) were identified, which were found to be highly expressed in appressoria and under the control of the PMK1 MAPK. In addition, *gas1* and *gas2* were both found to be required for efficient appressorium formation and penetration (Xue *et al*., 2002). We therefore searched for *B. cinerea* genes similar to *gas1* and *gas2*. Although several genes were found that encoded proteins with similarities between 35% and 40% to *M. grisea* Gas1, one gene, called *Bc-gas2*, was found to encode a protein with 68% similarity to *M. grisea* Gas2. As *B. cinerea gas2* appeared to represent an orthologue of *M. grisea gas2*, it was chosen for further analysis. It encodes a predicted protein of 285 amino acids, with a probable N-terminal signal peptide of 19 amino acids. Although Mg-Gas2 also contains a predicted signal peptide, green fluorescent protein (GFP) fusions indicated that it is located in the cytosol (Xue *et al*., 2002). In order to test the role of Bc-Gas2 in pathogenesis, Δ*gas2* knock-out mutants were generated. Five independent Δ*gas2* transformants were obtained and confirmed by PCR and Southern analysis (data not shown).

All Δ*gas2* mutants showed normal growth, germination and penetration (data not shown). When plant infection tests were performed, variable phenotypes of the different Δ*gas2* mutants

	wt	Δste12	Δste12 + ΔE4	Δste12 + fs	wt + ΔE4		
					0	1	5
RT-PCR fs ΔE4 fold increase 2,5 2,0 1,5 1,0 0,5 0,0	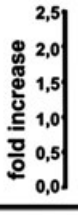	- -				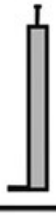	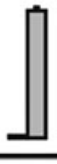
RT-PCR fs [% of wt fs]	100	0	0	166	18	3	3
RT-PCR ΔE4 [% of wt fs]	66	0	58	0	86	224	175
increased melanization	-	+	-	-	-	+	+
infection (days until lesion formation)	1	2	1	1	2	-	3
sclerotia formation (sclerotia per plate)	> 50	-	-	> 50	> 50	< 3	< 3

Fig. 7 *Ste12* transcript levels and phenotypes of *Botrytis cinerea* transformants expressing full-sized (fs) *ste12* and *ste12*ΔE4 transcripts. RNAs were isolated from germinated spores at 3 h post-inoculation (hpi). Sclerotia formation was tested under standard conditions [Gamborg's B5 medium, 20 °C, darkness, 10 days post-inoculation (dpi)]. The smaller transcript can also complement the Δ*ste12* defects, except for sclerotia formation. Overexpression of *ste12*ΔE4 in the wild-type (wt) background leads to increased melanization and inhibition of infection and sclerotia formation, similar to the defects resulting from *ste12* deletion.

were observed. Although one was strongly reduced in lesion formation on tomato leaves (lesion expansion rate of less than 1 mm/day), three Δ*gas2* mutants showed a slightly reduced infection (3.4 ± 0.4 mm/day). One mutant, however, induced lesions with the same speed as the wt strain (4.5 ± 0.1 and 4.7 ± 0.1 mm/day, respectively). Although these data are not completely consistent, we decided not to analyse further transformants, but concluded that Bc-Gas2 plays either no or only a minor role in the pathogenesis of *B. cinerea*.

We tested whether the disruption of the MAPK cascade leads to altered expression of putative target genes during early germination stages. We therefore measured the transcript levels of *gas2* in the wt, Δ*bmp1* and Δ*ste12* mutants using the genes encoding elongation factor 1α and actin as references. In the wt, *gas2* transcript levels were very low in non-germinated conidia, but increased strongly during the first hours of germination (Fig. 8). During infection of tomato leaves, transcript levels of *gas2* were lower than in saprophytic mycelium. In the Δ*bmp1* and Δ*ste12* mutants, *gas2* transcript levels were extremely low during all developmental stages tested, indicating that *gas2* expression is controlled by both Bmp1 and Ste12.

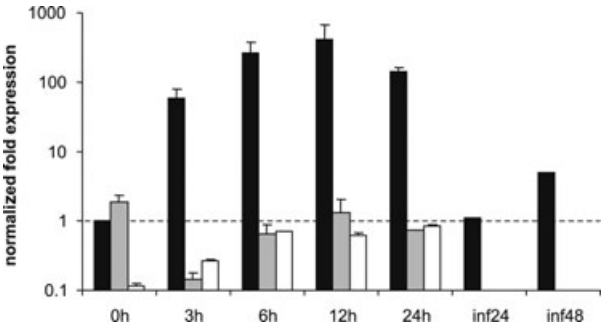

Fig. 8 Expression of *gas2* during germination and hyphae growth in Gamborg's B5 medium on apple wax and during infection of tomato leaf tissue (inf) at 24 and 48 h post-inoculation in *Botrytis cinerea* wild-type (wt) (black), Δ*bmp1* mutant (grey) and Δ*ste12* mutant (white). The strong increase in *gas2* expression in the wt during germination is not observed in the Δ*bmp1* and Δ*ste12* mutants.

DISCUSSION

In this study, we have investigated the role of several components of the BMP1 MAPK cascade, including the putative downstream transcription factor Ste12 and the BMP1 MAPK-regulated gene *gas2*. Structural and functional connections between various MAPK cascade components have already been established in *M. grisea* (Zhao *et al*., 2005, 2007). Similarly, all *B. cinerea* mutants defective in Ste11, Ste7 and BMP1, as well as in the adaptor protein Ste50, showed very similar phenotypes. The vegetative growth of the *B. cinerea* MAPK mutants was reduced, as indicated by less-developed aerial mycelium and slower radial expansion, in particular on minimal medium. In MAPK mutants of *Cochliobolus heterostrophus* and *Fusarium graminearum*, reduced aerial mycelium formation has also been described

(Jenczmionka *et al*., 2003; Lev *et al*., 1999), whereas, in MAPK mutants of *M. grisea*, *P. teres* and *C. lagenarium*, vegetative growth is unaffected (Ruiz-Roldan *et al*., 2001; Takano *et al*., 2000; Xu and Hamer, 1996). Under conditions of high osmolarity, growth inhibition of all *B. cinerea* MAPK mutants was similar to the wt. This is different to the phenotypes of Δ*ste11* mutants in yeast and *M. grisea* Δ*mst11* mutants, which are hypersensitive to high-osmolarity conditions (Ramezani-Rad, 2003; Zhao *et al*., 2005). Yeast Ste11 and, possibly, *M. grisea* Mst11 are components of the high-osmolarity MAPK signalling pathway, but this does not seem to be the case for *B. cinerea*.

In addition to their reduced vegetative growth, the *B. cinerea* MAPK mutants also showed slightly reduced sporulation efficiency (data not shown) and formed smaller conidiospores, correlated with a smaller number of nuclei per spore. Defects in conidiation have been described for other MAPK mutants. In *P. teres*, abnormally shaped conidiophores and a complete loss of conidia formation have been described (Ruiz-Roldan *et al*., 2001). A lack of conidia has also been reported for Δ*chk1* mutants of *Co. heterostrophus*, and reduced conidiation has been observed for *C. lagenarium* and *F. graminearum* MAPK mutants (Jenczmionka *et al*., 2003; Lev *et al*., 1999; Takano *et al*., 2000).

Similar to the phenotype of Δ*bmp1*, the other MAPK mutants were unable to germinate on hydrophobic surfaces in water. As described previously, this defect appears to be a result of the loss of hydrophobic surface recognition (Doehlemann *et al*., 2006). Similar germination defects of Fus3/Kss1-type MAPK mutants have been reported up to now only for *C. lagenarium* (Yamauchi *et al*., 2004). None of the *B. cinerea* MAPK mutants were able to form sclerotia (which serve as both resting and female sexual reproduction structures), but instead showed excessive production of microconidia. In *Sclerotinia sclerotiorum*, the MAPK Smk1 has also been shown to be required for sclerotia formation (Chen *et al*., 2004). Defects in sexual reproduction have similarly been described for the non-sclerotia-forming *Co. heterostrophus* and *C. lagenarium*, but not for *M. grisea* (Lev *et al*., 1999; Takano *et al*., 2000; Xu and Hamer, 1996). This demonstrates that fungi have recruited conserved signalling pathways for the regulation of specific functions, such as hydrophobic surface-induced germination and sclerotia formation in *B. cinerea*.

All *B. cinerea* MAPK cascade mutants were almost completely non-pathogenic, being unable to invade and colonize plant tissue. On tomato leaves or *Gerbera* petals, they induced only scattered necrotic spots within the inoculation site. Mutant hyphae showed straight elongation on the host surface and no penetration attempts were observed. In wounded apple fruits, strongly reduced lesions were formed. Either a loss or strong reduction in pathogenicity has been reported for all Fus3/Kss1-type MAPK mutants of plant pathogenic fungi published so far (Zhao *et al*., 2007). This phenomenon is probably correlated with the inability of the mutant hyphae to undergo morphological and physiological changes that are required for surface recognition, penetration and colonization of host tissue.

By means of MAPK phosphorylation assays, protein–protein interaction studies via a yeast two-hybrid system and the analysis of mutants expressing a dominant active Mst7, the order of the MAPK cascade components Mst11–Mst7–PMK1 has been confirmed in *M. grisea* (Zhao *et al*., 2005). To test whether this is similar for the *B. cinerea* MAPK cascade, a dominant active allele of Bc-*ste7* was transformed into *B. cinerea* wt and the Δ*ste11* mutant. Generally, the phenotypes of the *ste7*^{DA} transformants did not differ strongly from those of the parent strains, except for a reduction in sugar-induced germination, which appeared to correlate with the expression levels of the dominant active allele. The only positive effect of the introduced *ste7*^{DA} allele was observed in the Δ*ste11* mutants, which regained, with a low but reproducible rate (up to 3%), the ability to germinate on hydrophobic surfaces in water, which was never observed in Δ*ste11* mutants. Because the defects of the Δ*ste11* mutants with regard to appressoria formation and infection were not repaired by *ste7*^{DA}, we conclude that the dominant active allele, in contrast with the situation in *M. grisea*, is unable to activate Bmp1 by phosphorylation.

Ste12 has been shown to be required for infection in *M. grisea*, two *Colletotrichum* spp. and *Cr. parasitica* (Deng *et al*., 2007; Hoi *et al*., 2007; Park *et al*., 2002). The *B. cinerea* Δ*ste12* mutants constructed in this study showed the accumulation of a dark pigment in hyphal aggregates, which has not been observed in other fungal *ste12* mutants. Doss *et al*. (2003) have identified melanin in the extracellular matrix of *B. cinerea* wt germlings, which are nevertheless not apparently pigmented. Evidence for increased melanization in parts of the mycelium of Δ*ste12* mutants was confirmed by inhibitor treatments, which led to the accumulation of coloured melanin precursors. In addition, mycelial growth on minimal medium differs from that observed in the wt. In contrast with the MAPK cascade mutants, Δ*ste12* conidia germinated normally and were still able to invade and colonize host tissue. However, the penetration efficiency was very low and lesion expansion in infected tomato leaves was retarded and reduced. Although it was not possible to observe microscopically, we assume that the penetration of tomato leaves possibly occurred from the mycelium via infection cushions (Williamson *et al*., 2007). Reduced lesion formation was also described for *Cr. parasitica*, which does not form appressoria during host invasion. Infectious hyphae of a *Cp-ste12* mutant showed reduced invasion of the bark of chestnut stems and caused smaller cankers than the wt (Deng *et al*., 2007). Similar mutants in *M. grisea*, *C. lagenarium* and *C. lindemuthianum* were completely unable to colonize intact host tissue caused by defects in penetration peg formation, although their appressoria seemed to be normal in turgor pressure and

ultrastructure (Hoi *et al*., 2007; Park *et al*., 2004; Tsuji *et al*., 2003). In *M. grisea*, rearrangement of the cytoskeleton is observed during penetration. Park *et al*. (2004) showed that microtubule reorganization in mature appressoria is disturbed in Δ*mst12* mutants, which possibly leads to penetration defects. We assume that the inability to achieve appropriate cytoskeleton reorganization might also be responsible for the penetration defects of *ste12* mutants in other fungi. Thus, penetration mediated by the transcription factor Ste12 is essential for fungi to form highly differentiated, melanized appressoria, whereas fungi that form structurally less developed appressoria or invasion hyphae might partially overcome the penetration defect.

Ste12 proteins from filamentous fungi contain, close to their C-termini, two tandem C_2H_2 zinc finger domains which are absent in Ste12 of ascomycetous yeasts. In *C. lagenarium* Ste12, an alternative splicing mechanism has been described that eliminates one of the two zinc finger domains by exon skipping. All *ste12* genes of filamentous ascomycetes, but not those of basidiomycetes, have two short introns in the region encoding the zinc finger domains, which could allow alternative splicing. Indeed, two *ste12* transcripts were detected in *B. cinerea*, and the levels of the smaller transcript were lower than those of the full-sized transcript in all analysed growth stages. The expression of either transcript was able to complement the defects of a Δ*ste12* strain, except for the formation of sclerotia, which could not be complemented by the *ste12*Δ*E4* transcript. This was in contrast with the situation in *C. lindemuthianum*, in which the smaller transcript exerted a dominant negative effect on invasive growth (Hoi *et al*., 2007). However, a dominant negative effect on infection was also observed when the *ste12*Δ*E4* transcript was expressed in the *B. cinerea* wt strain. These negative effects were more severe in those transformants in which the *ste12*Δ*E4* transcript was overexpressed. Thus, the truncated *ste12*Δ*E4* transcript is almost completely functional, but increased levels of *ste12*Δ*E4* seem to inhibit infection-related morphogenesis. Therefore, our data indicate that the truncated *ste12* transcript has some unusual properties, but its exact role remains unresolved.

In *M. grisea*, two genes (*gas1* and *gas2*) were identified that were highly expressed in appressoria and dependent on the PMK1 MAPK (Xue *et al*., 2002). Gas1 and Gas2 belong to a family of proteins that were first described to be highly expressed during the early stages of infection in the powdery mildew fungus *Blumeria graminis* (Grell *et al*., 2003). Gas1- and Gas2-like proteins have been found only in filamentous ascomycetes. *Botrytis cinerea gas2* was selected for further studies because of its strong similarity to *M. grisea gas2* and *Bl. graminis Egh16h1*, and the stage-specific expression of these genes. Knock-out mutants did not reveal clear evidence for any function of *gas2* in *B. cinerea*. The inconsistency of the results of the plant infection tests, obtained with five independent, putatively isogenic Δ*gas2* knock-out transformants, was unusual. Until now, *B. cinerea* knock-out mutants for several genes have been constructed in our laboratory, and most of them have revealed similar phenotypes of independent transformants. Nevertheless, the results of the infection tests altogether argue against a significant role of *gas2* in plant infection. In the wt, *gas2* expression was very low in resting spores, reached maximum levels during late stages of germination (12 hpi) and decreased during the mycelium growth stage (24 hpi). During infection, *gas2* expression remained low. Therefore, in contrast with *M. grisea* and *Bl. graminis*, the expression of *gas2* is not confined to the early stages of germination and infection in *B. cinerea*. In Δ*bmp1* and Δ*ste12* mutants, *gas2* expression was drastically reduced, clearly indicating that *gas2* is controlled by both BMP1 MAPK and Ste12. Our results indicate that Ste12 might indeed be one of several downstream components of the BMP1 MAPK cascade. This is supported by preliminary microarray data, which indicated that a large number of genes were down-regulated during germination in both the Δ*bmp1* and Δ*ste12* mutants (A. Schamber *et al*., in preparation).

EXPERIMENTAL PROCEDURES

Fungal growth conditions and transformation

Botrytis cinerea strain B05.10 was used as wt for the studies. Cultivation and spore production were performed on TMA as described previously (Doehlemann *et al*., 2006). Growth tests were also performed on HA and on GB5 minimal medium containing 50 mM glucose (Rui and Hahn, 2007). Transformation of *B. cinerea* was performed as described previously (Reis *et al*., 2005), except that transformed protoplasts were spread immediately onto selective plates using 50 μg/mL hygromycin or 60 μg/mL nourseothricin. Transformants were transferred to HA agar supplemented with hygromycin (70 μg/mL) or nourseothricin (85 μg/mL). After single spore isolation, transformants were cultivated without selection on TMA. For the inhibition of melanin biosynthesis, strains were grown on HA agar plates supplemented with 10 μg/mL tricyclazole (Sigma-Aldrich, St Louis, MO, USA).

Tests for germination, penetration and plant infection

Germination tests on artificial substrates and penetration assays on onion epidermal cells were performed as described by Doehlemann *et al*. (2006). For infection tests, conidia were harvested as described previously (Doehlemann *et al*., 2006). They were suspended in GB5 basal salt mixture supplemented with 25 mM glucose and 10 mM KH_2PO_4 (pH 5.5) at a concentration of 10^5 conidia/mL, and preincubated for 2 h at room temperature. Detached leaves were inoculated with 20-μL droplets of spore

suspension, and incubated at 20 °C in a humid box at ambient light conditions. Inoculation of wounded apples was performed as described previously (Rui and Hahn, 2007). Each experiment was repeated at least three times with duplicates in each experiment. Error bars were calculated as standard error.

For the microscopic evaluation of infection development on tomato leaves, cell layers from the reverse side of the inoculated leaves were scratched off with a razor blade. The infected area was cut from the leaf, the tissue bleached by incubation for 40 min at 60 °C in 50% ethanol and 50% glacial acetic acid, transferred to 75% lactic acid for at least 20 h, and fixed on a microscope slide. Staining was performed with lactophenol–trypan blue (phenol–water–lactic acid–trypan blue = 1 : 1 : 1 : 0.1) for 10 min, followed by a short wash in lactic acid. For low-temperature scanning electron microscopy (LTSEM), *B. cinerea* conidia were inoculated onto bean leaves as described above for tomato leaves. LTSEM was performed as described by Kucheryava *et al*. (2008).

Nucleic acid manipulations and sequence data analysis

Isolation and manipulations of RNA and DNA were performed using standard protocols (Sambrook *et al*., 1989). A list of primers used in this study is shown in Table S1. Gene annotations were checked by comparing the predicted proteins with homologues of other fungi. Erroneous automatic annotations were identified, confirmed by sequencing and corrected for *ste11* (FJ374679) and *ste12* (FJ374678). Protein sequences were aligned using the CLUSTAL X algorithm (Thompson *et al*., 1997), and manual corrections were performed with the GeneDoc editor (Nicholas *et al*., 1997).

Quantitative RT-PCR was performed using the MyIQ Real Time PCR Cycler (Bio-Rad, Munich, Germany). Fungal RNA was isolated with the RNeasy Plant Mini Kit (Qiagen, Hilden, Germany). One microgram of RNA was reverse transcribed into first-strand cDNA with oligo(dT) primers using a Verso cDNA Kit from Thermo Fisher Scientific (Epsom, Surrey, UK), and subsequently used for RT-PCR. The expression of genes was calculated by the $2^{-\Delta\Delta CT}$ method from Livak and Schmittgen (2001). Transcript levels were normalized against the expression levels of the housekeeping genes encoding elongation factor 1α and actin, and shown as 'normalized fold expression' relative to the expression in ungerminated conidia. Means of two biological replicates, with two technical replicates each, are shown. Error bars indicate standard errors.

Disruption of *B. cinerea ste11*, *ste7*, *ste50*, *ste12* and *gas2* genes

Constructs employed for gene disruptions were created using an inverse PCR strategy described in Doehlemann *et al*. (2006). For the generation of the knock-out constructs, primers Bst11-KO1/Bst11-KO4 were used for ste11, primers Bst7-KO1/Bst7-KO4 for ste7, primers Bst50-KO1/Bst50-KO4 for ste50, primers KO-Bst12-1/KO-Bst12-4 for ste12 and primers Bcgas2-1/Bcgas2-2 for gas2.

For complementation of the Δ*ste12* mutant, a 4136-bp genomic fragment containing the *ste12* gene, including 1190 bp upstream of the putative start codon and 543 bp downstream of the putative stop codon, was amplified using primers Ste12-K1 and KO-Bst12-2. The fragment was co-transformed into the Δ*ste12* mutant with the *Hin*dIII linearized plasmid pNR2 carrying a nourseothricin resistance cassette (Hayashi *et al*., 2002). Several nourseothricin-resistant transformants were obtained, all of which were hygromycin sensitive, as a result of homologous replacement of the deletion construct containing the hygromycin cassette by the complementing wt *ste12* fragment.

Southern hybridization was used to confirm knock-out and complemented strains. For Δ*ste11*, *Eco*RV/*Xho*I double digestion led to hybridization bands of 3031 bp for wt and 5299 bp for the knock-out strain; the probe was amplified using primers BcSte11-SO1/Bst11-KO3. For Δ*ste7*, *Eco*RI digestions led to hybridization signals of 2617 bp for wt and 2102 bp for the knock-out strain; the probe was amplified using primers BcSte7-SO1/Bst7-KO3. For Δ*ste50* confirmation, genomic DNA was digested with *Bam*HI/*Eco*RV, leading to hybridization bands of 2169 bp for wt and 3532 bp for the knock-out strain; the probe was amplified with primers BcSte50-SO1/Bst50-KO3. For Δ*ste12* confirmation, genomic DNA was digested with *Xho*I/*Bam*HI, resulting in hybridization bands of 4108 bp for wt and 2186 bp for the knock-out strain; the probe was amplified with primers BcSte12-SO1/KO-Bst12-4.

Construction of *ste7*^{DA}

ste7^{DA} was constructed by site-directed mutagenesis. Using primers Ste7-KA1a and Ste7-TAG-NotI, a 2599-bp genomic fragment was amplified, digested with *Not*I and ligated into a *Not*I-digested pLOB derivative lacking the *oliC* promoter region and the hygromycin resistance cassette. The resulting plasmid was used for site-directed mutagenesis with the Quick Change Site Directed Mutagenesis Kit (Stratagene, La Jolla, CA, USA), employing the complementary mutagenesis primers Bst7-mut and Bst7-mut.inv. These primers changed the sequence within the *ste7* coding region from TCAGTGGCAGACACCTTC to GATGTGGCAGACGAATTC, resulting in a change in the Ste7 amino acid sequence from 219-SVADT-223 (Ste7) to 219-DVADE-223 (Ste7^{DA}), and the introduction of a new *Eco*RI site. From the resulting plasmid, *ste7*^{DA}, including its promoter region, was amplified using primers Bst7-KA1a and Bst7-TAG-*Not*I. This fragment was used for co-transformation with the nourseothricin resistance plasmid pNR2 (Hayashi *et al*., 2002) into the B05.10 wt and the Δ*ste11* mutant. For confirmation of the transfor-

mants, PCR with primers Bst7-S1/Bst7-S2/Bst7-S3 and Bst7-S4/Bst7-S5 was performed (Fig. 3B). Bst7-S3 binds only to the mutated region. Digestion of the PCR product Bst7-S4/Bst7-S5 with *Eco*RI allowed further confirmation of the mutation through the newly generated *Eco*RI site. To confirm the expression of *ste7*^{DA}, RT-PCR was conducted using primers Bst7-S4/Bst7-S3, resulting in a product of 166 bp, and primers Bst7-S4/Bst7-S5 for the detection of wt *ste7* as a positive control.

Complementation of wt and Δ*ste12* with *ste12ΔE4* and the full-sized *ste12* allele

The complete *ste12* gene, including the 1190-bp upstream and 538-bp downstream sequences of the coding region, was amplified with primers ste12-K1 and ste12-KO2 and cloned into pBS+ (Stratagene, La Jolla) using *Xba*I and *Bam*HI sites, resulting in pBS-*ste12*. The genomic *ste12* region covering intron 3, exon 3 and intron 4 were replaced by cDNA obtained from strain B05.10. Using primers ste12-RTfor3 and ste12-RTrev, products of both splice variants were obtained (811 bp and 895 bp), separated by gel extraction and introduced through *Bgl*II and *Oli*I sites into pBS-*ste12*. The resulting plasmids were linearized with *Xba*I and used for co-transformation with pNR2 containing the nourseothricin resistance cassette. The Δ*ste12* mutant was transformed with both constructs, whereas the wt was only transformed with *ste12ΔE4*. PCR analysis with three transformants for each transformed strain with primers Ste12-RTfor_c/Ste12-RTrev_c showed that the constructs were integrated ectopically. RT-PCR experiments confirmed that the introduced constructs were expressed in all transformants. For RT-PCR amplification of only the full-sized *ste12* transcript, primers Ste12-RTfor_c and Ste12-RTrev_b were used. For amplification of only the *ste12ΔE4* transcript, primers Ste12-RTfor_c and Ste12-RTrev_spanE4 were used.

The GENBANK accession numbers were as follows: *Bc-ste7* (EDN20614), *Bc-ste11* (FJ374679), *Bc-ste50* (EDN27521), *Bc-ste12* (FJ374678), *Bc-gas2* (EDN19732), Bc-elongation factor 1-α (XP_001551786), Bc-actin (XP_001553368).

ACKNOWLEDGEMENTS

We are grateful to Anna Hummrich for help with *ste12* expression analysis, Sara Mazzotta for construction of the Δ*gas2* mutants, Carsten Rupp for microscopy of infected tomato leaves and Gunther Döhlemann for valuable discussions. This work was supported by the German Science Foundation (DFG; HA1486/5).

REFERENCES

Bell, A.A. and Wheeler, M.H. (1986) Biosynthesis and functions of fungal melanins. *Annu. Rev. Phytopathol.* **24**, 411–451.

Chen, C., Harel, A., Gorovoits, R., Yarden, O. and Dickman, M.B. (2004) MAPK regulation of sclerotial development in *Sclerotinia sclerotiorum* is linked with pH and cAMP sensing. *Mol. Plant–Microbe Interact.* **17**, 404–413.

Chou, S., Lane, S. and Liu, H. (2006) Regulation of mating and filamentation genes by two distinct Ste12 complexes in *Saccharomyces cerevisiae*. *Mol. Cell. Biol.* **26**, 4794–4805.

Deng, F., Allen, T.D. and Nuss, D.L. (2007) Ste12 transcription factor homologue CpST12 is down-regulated by hypovirus infection and required for virulence and female fertility of the chestnut blight fungus *Cryphonectria parasitica*. *Eukaryot. Cell* **6**, 235–244.

Doehlemann, G., Berndt, P. and Hahn, M. (2006) Different signalling pathways involving a Gα protein, cAMP and a MAP kinase control germination of *Botrytis cinerea* conidia. *Mol. Microbiol.* **59**, 821–835.

Doss, R.P., Deisenhofer, J., Krug von Nidda, H.-A., Soeldner, A.H. and McGuire, R.P. (2003) Melanin in the extracellular matrix of germlings of *Botrytis cinerea*. *Phytochemistry*, **63**, 687–691.

Grell, M.N., Mouritzen, P. and Giese, H. (2003) A *Blumeria graminis* gene family encoding proteins with a C-terminal variable region with homologues in pathogenic fungi. *Gene*, **311**, 181–192.

Gustin, M.C., Albertyn, J., Alexander, M. and Davenport, K. (1998) MAP kinase pathways in the yeast *Saccharomyces cerevisiae*. *Microbiol. Mol. Biol. Rev.* **62**, 1264–1300.

Hayashi, K., Schoonbeek, H.J. and De Waard, M.A. (2002) Expression of the ABC transporter BcatrD from *Botrytis cinerea* reduces sensitivity to sterol demethylation inhibitor fungicides. *Pestic. Biochem. Physiol.* **73**, 110–121.

Hoi, J.W., Herbert, C., Bacha, N., O'Connell, R., Lafitte, C., Borderies, G., Rossignol, M., Rougé, P. and Dumas, B. (2007) Regulation and role of a STE12-like transcription factor from the plant pathogen *Colletotrichum lindemuthianum*. *Mol. Microbiol.* **64**, 68–82.

Jenczmionka, N.J., Maier, F.J., Loesch, A.P. and Schäfer, W. (2003) Mating, conidiation and pathogenicity of *Fusarium graminearum*, the main causal agent of the head-blight disease of wheat, are regulated by the MAP kinase gpmk1. *Curr. Genet.* **43**, 87–95.

Kucheryava, N., Bowen, J.K., Sutherland, P.W., Conolly, J.J., Mesarich, C.H., Rikkerink, E.H., Kemen, E., Plummer, K.M., Hahn, M. and Templeton, M.D. (2008) Two novel *Venturia inaequalis* genes induced upon morphogenetic differentiation during infection and *in vitro* growth on cellophane. *Fungal Genet. Biol.* **45**, 1329–1339.

Lev, S., Sharon, A., Hadar, R., Ma, H. and Horwitz, B.A. (1999) A mitogen-activated protein kinase of the corn leaf pathogen *Cochliobolus heterostrophus* is involved in conidiation, appressorium formation, and pathogenicity: diverse roles for mitogen-activated protein kinase homologs in foliar pathogens. *Proc. Natl. Acad. Sci. USA*, **96**, 13 542–13 547.

Li, D., Bobrowicz, P., Wilkinson, H.H. and Ebbole, D.J. (2005) A mitogen-activated protein kinase pathway essential for mating and contributing to vegetative growth in *Neurospora crassa*. *Genetics*, **170**, 1091–1104.

Livak, K.J. and Schmittgen, T.D. (2001) Analysis of relative gene expression data using real-time quantitative PCR and the $2^{-\Delta\Delta CT}$ method. *Methods*, **25**, 402–408.

Mendgen, K., Hahn, M. and Deising, H. (1996) Morphogenesis and mechanisms of penetration by plant pathogenic fungi. *Annu. Rev. Phytopathol.* **34**, 367–386.

Nicholas, K.B., Nicholas Jr, H.B. and Deerfield II, D.W. (1997) GeneDoc: analysis and visualization of genetic variation. *EMBNET News*, **4**, 1–4.

Park, G., Xue, C., Zheng, L., Lam, S. and Xu, J.-R. (2002) MST12 regulates infectious growth but not appressorium formation in the rice blast fungus *Magnaporthe grisea*. *Mol. Plant–Microbe Interact.* **15**, 183–192.

Park, G., Bruno, K.S., Staiger, C.J., Talbot, N.J. and Xu, J.R. (2004) Independent genetic mechanisms mediate turgor generation and penetration peg formation during plant infection by the rice blast fungus. *Mol. Microbiol.* **53**, 1695–1707.

Park, G., Xue, C., Zhao, X., Kim, Y., Orbach, M. and Xu, J.R. (2006) Multiple upstream signals converge on the adaptor protein Mst50 in *Magnaporthe grisea*. *Plant Cell*, **18**, 2822–2835.

Ramezani-Rad, M. (2003) The role of adaptor protein Ste50-dependent regulation of the MAPKKK Ste11 in multiple signalling pathways of yeast. *Curr. Genet.* **43**, 161–170.

Reis, H., Pfiffi, S. and Hahn, M. (2005) Molecular and functional characterization of a secreted lipase from *Botrytis cinerea*. *Mol. Plant Pathol.* **6**, 257–267.

Rui, O. and Hahn, M. (2007) The *Botrytis cinerea* hexokinase, Hxk1, but not the glucokinase, Glk1, is required for normal growth and sugar metabolism, and for pathogenicity on fruits. *Microbiology*, **153**, 2791–2802.

Ruiz-Roldan, M.C., Maier, F.J. and Schäfer, W. (2001) PTK1, a mitogen-activated-protein kinase gene, is required for conidiation, appressorium formation, and pathogenicity of *Pyrenophora teres* on barley. *Mol. Plant–Microbe Interact.* **14**, 116–125.

Sambrook, J., Fritsch, E.F. and Maniatis, T. (1989) *Molecular Cloning: A Laboratory Manual*. New York: Laboratory Press, Cold Spring Harbor.

Schumacher, J., Kokkelink, L., Huesmann, C., Jimenez-Teja, D., Collado, I.G., Barakat, R., Tudzynski, P. and Tudzynski, B. (2008) The cAMP-dependent signaling pathway and its role in conidial germination, growth and virulence of the gray mold *Botrytis cinerea*. *Mol. Plant–Microbe Interact.* **21**, 1443–1459.

Takano, Y., Kikuchi, T., Kubo, Y., Hamer, J.E., Mise, K. and Furusawa, I. (2000) The *Colletotrichum lagenarium* MAP kinase gene *cmk1* regulates diverse aspects of fungal pathogenesis. *Mol. Plant–Microbe Interact.* **13**, 374–383.

Thompson, J.D., Gibson, T.J., Plewniak, F., Jeanmougin, F. and Higgins, D.G. (1997) The ClustalX windows interface: flexible strategies for multiple sequence alignment aided by quality analysis tools. *Nucleic Acids Res.* **24**, 4876–4882.

Tsuji, G., Fujii, S., Tsuge, S., Shiraishi, T. and Kubo, Y. (2003) The *Colletotrichum lagenarium* Ste12-like gene CST1 is essential for appressorium penetration. *Mol. Plant–Microbe Interact.* **16**, 315–325.

Vallim, M.A., Miller, K.Y. and Miller, B.L. (2000) Aspergillus SteA (Sterile12-like) is a homeodomain-C_2/H_2-Zn^{+2} finger transcription factor required for sexual reproduction. *Mol. Microbiol.* **36**, 290–301.

Williamson, B., Tudzynski, B., Tudzynski, P. and van Kan, J.A.L. (2007) Pathogen profile. *Botrytis cinerea*: the cause of grey mould disease. *Mol. Plant Pathol.* **8**, 561–580.

Woloshuk, C.P., Wolkow, P.M. and Sisler, H.D. (1981) The effect of three fungicides, specific for the control of rice blast disease, on the growth and melanin biosynthesis by *Pyricularia oryzae*. *Cav. Pestic. Sci.* **12**, 86–90.

Xu, J.R. and Hamer, J.E. (1996) MAP kinase and cAMP signaling regulate infection structure formation and pathogenic growth in the rice blast fungus *Magnaporthe grisea*. *Genes Dev.* **10**, 2696–2706.

Xue, C., Park, G., Choi, W., Zheng, L., Dean, R.A. and Xu, J.R. (2002) Two novel fungal virulence genes specifically expressed in appressoria of the rice blast fungus. *Plant Cell*, **14**, 2107–2119.

Yamauchi, J., Takayanagi, N., Komeda, K., Takano, Y. and Okuno, T. (2004) cAMP-PKA signaling regulates multiple steps of fungal infection cooperatively with Cmk1 MAP kinase in *Colletotrichum lagenarium*. *Mol. Plant-Microbe Interact.* **17**, 1355–1365.

Zhao, X. and Xu, J.R. (2007) A highly conserved MAPK-docking site in Mst7 is essential for Pmk1 activation in *Magnaporthe grisea*. *Mol. Microbiol.* **63**, 881–894.

Zhao, X., Kim, Y., Park, G. and Xu, J.R. (2005) A mitogen-activated protein kinase cascade regulating infection-related morphogenesis in *Magnaporthe grisea*. *Plant Cell*, **17**, 1317–1329.

Zhao, X., Mehrabi, R. and Xu, J.R. (2007) Mitogen-activated protein kinase pathways and fungal pathogenesis. *Eukaryot. Cell*, **6**, 1701–1714.

Zheng, L., Campbell, M., Murphy, J., Lam, S. and Xu, J.R. (2000) The BMP1 gene is essential for pathogenicity in the gray mold fungus *Botrytis cinerea*. *Mol. Plant–Microbe Interact.* **13**, 724–732.

SUPPORTING INFORMATION

Additional Supporting Information may be found in the online version of this article:

Fig. S1 Confirmation of *Botrytis cinerea* mitogen-activated protein kinase (MAPK) and *ste12* knock-out mutants by genomic Southern hybridization. (A) Confirmation of *B. cinerea* MAPK knock-out mutants. Total DNA was digested with *Eco*RI (*ste7*; lanes 1a–1d), *Xho*I + *Eco*RV (*ste11*; lanes 2a–2c) and *Bam*HI + *Eco*RV (*ste50*; lanes 3a–3b). DNA was derived from B05.10 wt (1a, 2a, 3a), and from Δ*ste7* (1b, 1c, 1d), Δ*ste11* (2b, 2c) and Δ*ste50* (3b) mutant strains. The sizes of the hybridization signals are in agreement with the predictions (see Experimental procedures). (B) Confirmation of a Δ*ste12* mutant. DNA from B05.10 (a), Δ*ste12* mutant (b) and a complemented mutant Δ*ste12-c* (c) was digested with *Xho*I + *Bam*HI and hybridized to a *ste12* fragment (see Experimental procedures). In the Δ*ste12-c* strain, the introduced wt *ste12* copy had replaced the knock-out construct, including the hygromycin cassette. The presence of the nourseothricin cassette was proven by polymerase chain reaction (PCR) and growth of the transformants on HA containing 85 μg/mL nourseothricin (data not shown).

Fig. S2 Growth rate, conidia dimensions, nuclei number and germination rate of wt and mitogen-activated protein kinase (MAPK) mutants. (A) Radial growth rates of the mutants relative to the B05.10 wt strain on different media. Growth rates of B05.10 (mm/day) were 11.8 ± 0.3 on TMA, 9.9 ± 0.2 on HA and 8.6 ± 0.9 on Gamborg's B5 (GB5) agar. (B) Dimensions, number

of nuclei and germination rates of wt and MAPK mutant conidia. The shape was determined as length/width (*l*/*w*). The volume of wt spores was 327 ± 22 fl.

Fig. S3 Semi-quantitative, real-time polymerase chain reaction (RT-PCR) for the confirmation of *ste7*^{DA} expression with primers Bst7-S4/Bst7-S3 amplifying 166 bp exclusively within *ste7*^{DA} but not within *ste7*.

Table S1 Oligonucleotide primers used in this study.

Please note: Wiley-Blackwell are not responsible for the content or functionality of any supporting materials supplied by the authors. Any queries (other than missing material) should be directed to the corresponding author for the article.

